XLA-200: the Third-Generation ArF MOPA Light Source for Immersion Lithography

Toshihiko Ishihara, Robert Rafac, Wayne Dunstan, Fedor Trintchouk, Christian Wittak, Richard Perkins, Robert Bergstedt, and Walter Gillespie

Cymer, Inc.
17075 Thornmint Ct., San Diego, CA 92127 USA

ABSTRACT

The first generation MOPA-based ArF laser XLA-100 was introduced in January 2003 in response to the needs of high NA ArF scanners for higher power and narrower spectral bandwidth. The second generation product XLA-105 was introduced in early 2004. This paper presents our third generation MOPA-based ArF laser product XLA-200 that is designed and engineered to meet the light source requirements of the ArF immersion lithography. It is expected to be used for 65-nm and 45-nm volume production of semiconductor devices.

The XLA-200 is capable of producing a 60W of ultra-line-narrowed 193nm light with the FWHM bandwidth of less than 0.15pm and the E95% integral bandwidth of less than 0.35pm. It features state-of-the-art on-board bandwidth metrology tool that measures E95% bandwidth as well as FWHM. Real-time accurate bandwidth information can be utilized for lithography exposure tool feedback control. The improved dual-chamber laser gas control ensures excellent bandwidth stability, which enables tighter CD control. Together with a lower cost of operation, the XLA-200 sets a new performance level for the dual chamber 193nm light source for microlithography.

Keywords: Excimer laser, 193nm light source, narrow bandwidth, immersion lithography

INTRODUCTION

The XLA-200 is a third generation master oscillator and power amplifier (MOPA) based ArF excimer laser for microlithography. The first generation ArF MOPA laser XLA-100 and the second generation XLA-105 have demonstrated the superior performance of the dual chamber MOPA ArF design over the single chamber design. A number of systems have already been installed in semiconductor fabs and are producing semiconductor devices in large volumes. Detailed discussions of the XLA ArF MOPA design and performance were presented in our previous papers.[1,2,3]

The XLA-200 is capable of producing a 15mJ pulse energy or 60W of line-narrowed ArF laser light at 4000Hz. The higher pulse energy is achieved by re-optimizing the balance between MO and PA laser gas pressures and employing new optical components with high damage thresholds. The XLA-200 can be configured to have a maximum pulse energy output ranging from 11.5 to 15mJ.

The FWHM bandwidth of the XLA-200 is typically 0.12pm, and the 95% integral bandwidth (E95%) is 0.25pm, a 25% improvement in FWHM and 30% improvement in E95% over the XLA-105. The better output spectrum is achieved by re-designing the line-narrowing module. Such narrow bandwidths allow scanner lens designers to create projection lenses with less CaF2 elements while still allowing increasing lens NA.[4]

As the spectral bandwidth becomes progressively smaller, one of the issues that the laser light source manufacturers come to face is that the standard etalon-based bandwidth metrology tools are deemed to be inadequate for accurately measuring extremely narrow bandwidths.[5] At the same time, E95% bandwidth information is becoming important for process control and accurate optical proximity corrections. The XLA-200 is equipped with a newly designed single-etalon-based on-board Bandwidth Analysis Module (BAM) that measures FWHM and E95% bandwidths with an accuracy that is comparable to that of a grating spectrometer, and it provides scanners with real time bandwidth

Optical Microlithography XVIII, edited by Bruce W. Smith,
Proceedings of SPIE Vol. 5754 (SPIE, Bellingham, WA, 2005)
0277-786X/05/$15 · doi: 10.1117/12.600075

measurements. Such accurate bandwidth measurements were previously only possible with a large, high resolution grating spectrometer.

The laser gas control processes and fluorine gas injection algorithm are redesigned for XLA-200. An ability to precisely control laser gas mixtures during the refill process and to stabilize fluorine concentrations during laser operation plays an important role in maintaining optical performance at higher levels. The new laser gas control provides stable optical performance over at least one hundred million pulses.

Polarization of the wafer exposing light can affect CD, especially of hyper NA scanners. Polarization effects have been studied theoretically and empirically for immersion lithography and also for conventional lithography processes, and scanners have been designed to make use of certain polarization effects to achieve better CDs.[6,7,8] For that reason, the light sources for hyper NA scanners must maintain minimum acceptable levels of polarization. The XLA-200 is capable of producing a highly polarized light even at the maximum output power of 60W.

Expected lifetimes of the PA chamber and major optical modules are extended for the XLA-200. The expected lifetime of the PA chamber is improved from 18Bpulses to 24Bpulses, the line-narrowing module (LNM) from 20 to 30Bpulses, and the line center analysis module (LAM) and bandwidth metrology module (BAM) from 20 to 30Bpulses. Thus, a 20% reduction in the cost of consumables (COC) has been achieved.

HIGHER OUTPUT POWER

The XLA-200 is capable of producing up to 60W of highly line-narrowed ArF laser light at 4000Hz, which is a 30% increase in maximum output power from the previous generation products. The XLA-200 can be configured as a 60W maximum output power system, a 46W maximum output power system, or anywhere in between. The 60W system has an output energy range from 11mJ to 15mJ, and the 46W system has an output energy range from 8.5mJ to 11.5mJ. Figure 1 shows system output energy vs high voltage curves of a new system, but optimized for two different output energy ranges. The XLA-200 pulse power module and discharge chambers operate reliably up to 1180V, which provides large energy overheads and thus ensures long chamber lives. Figure 2 is an example of the energy dose performance when optimized for a 60W maximum output power.

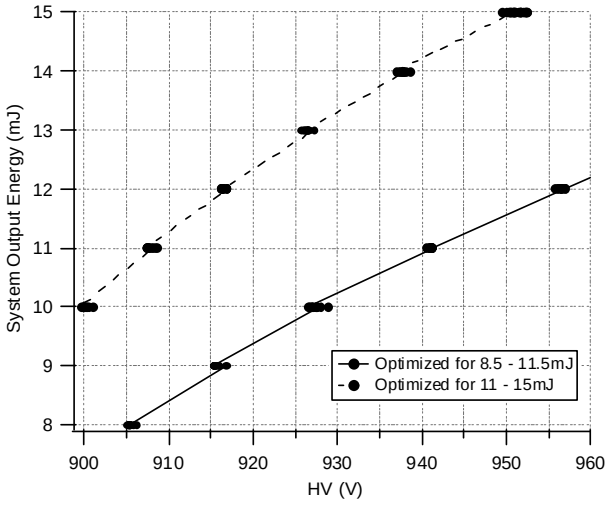

Figure 1: System output energy vs high voltage curves for a typical new system optimized for two different output energy ranges. Data were taken in a 75% duty cycle operation at 4000Hz.

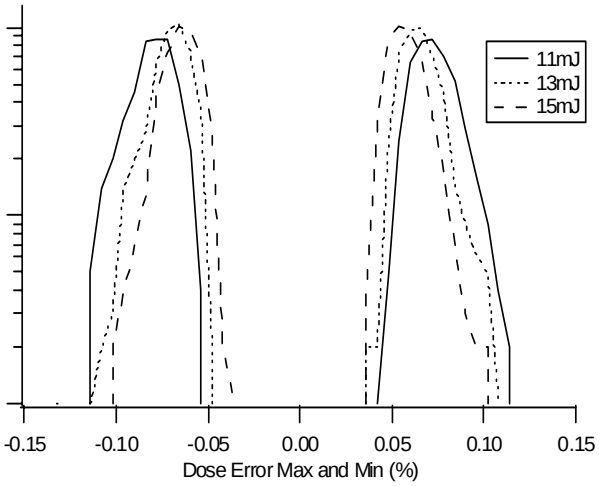

Figure 2: A Histogram of dose error maximum and minimum measured over 500 bursts in a 75% duty cycle operation. A 34-pulse trapezoidal window with 2-pulse leading and trailing slopes is used. The system is optimized for the 11 - 15mJ output energy range.

SPECTRAL BANDWIDTH IMPROVEMENT

The XLA-200 spectral bandwidth is typically 0.12pm in FWHM and 0.25pm in E95%. To achieve good bandwidth performance, considerations have to be made not only to the single pulse spectrum shape but also to the effect of wavelength stability on the apparent spectral bandwidth that points on the wafer surface see during exposure. The points on the wafer surface receive multiple laser pulses during exposure, the number of which is determined by scanning speed and laser pulse repetition rate. For instance, with the exposure time of 10msec at a 4000Hz pulse repetition rate, each point on the wafer surface sees 40pulses of laser light. Pulse-to-pulse fluctuation of center wavelength causes the apparent spectral profile to become wider than that of each individual laser pulse. The apparent spectral profile that a point on the wafer surface sees, $S(\lambda)$, can be written as

$$S(\lambda) = \sum_{i=0}^{n} s(\lambda - \Delta\lambda_i)$$

where $s(\lambda)$ is the single pulse spectral profile, $\Delta\lambda_I$ is the wavelength error of the i-th pulse, and n is the number of laser pulses that a point on the wafer surface sees, assuming that the single pulse spectral shape is consistent over the n pulses.

To quantitatively determine the effect of wavelength stability on the apparent spectral bandwidth, a simulation was performed using a Voigt function for the single pulse spectral profile and a Gaussian distribution for the center wavelength fluctuation. Voigt profiles with different FWHM and E95% values were convolved with the wavelength Gaussian distribution, and the results are plotted in Figures 3 and 4. Apparent spectral bandwidths degrade as wavelength sigma becomes larger. The effect of wavelength fluctuation becomes a more significant part of the bandwidth budget as the single pulse bandwidth is made smaller. For instance, the increase in FWHM of the single pulse spectrum with 0.08pm in FWHM and 0.25pm in E95% due to the wavelength sigma of 0.02pm is 0.015pm whereas that of the single pulse spectrum of 0.12pm in FWHM and 0.25pm in E95% due to the same 0.02pm wavelength sigma is only 0.01pm. A similar effect is seen on E95%.

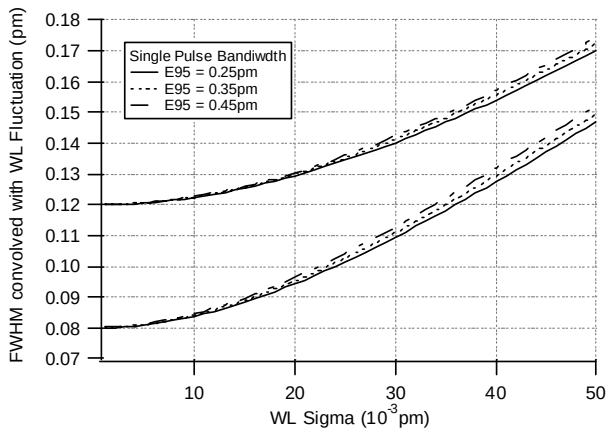

Figure 3: Effects of wavelength sigma on FWHM. Voigt profiles simulating laser single pulse spectra are convoluted with the Gaussian distributions with the sigma values up to 50fm, and the convoluted profiles are analyzed for FWHM bandwidth.

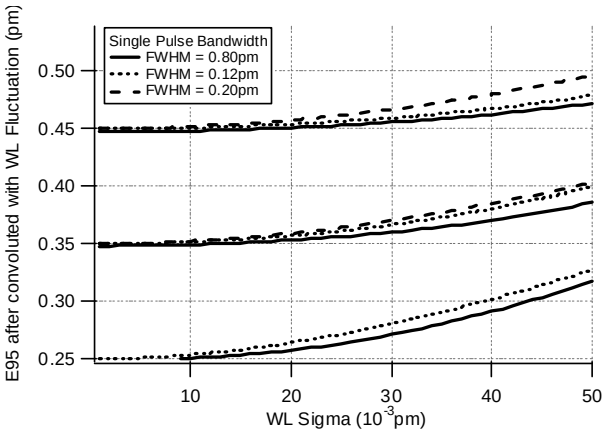

Figure 4: Effects of wavelength sigma on E95% Voigt profiles simulating laser single pulse spectra are convoluted with the Gaussian distributions with the sigma values up to 50fm, and the convoluted profiles are analyzed for E95% bandwidth.

In addition to the wavelength stability effect, other effects such as laser pulse repetition rate and duty cycle need to be carefully studied when determining apparent laser bandwidth performance. At certain repetition rates, bandwidths increase due to chamber acoustic phenomena. Optical loading of the components inside LNM varies with laser operation duty cycle, and affects single pulse spectral shape. The XLA-200 is equipped with a redesigned line-narrowing module to produce a narrower single pulse spectrum and a MO chamber that has less acoustic effects on spectral bandwidth than the first generation product. Our manufacturing process for line narrowing module includes an optimization procedure to minimize the difference between low duty cycle and high duty cycle bandwidths.

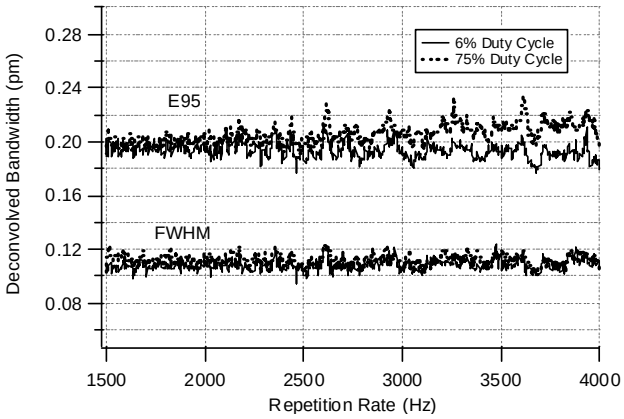

Figure 5: FWHM and E95% bandwidths vs repetition rate from 1500Hz to 4000Hz. Output pulse energy was set to 13mJ. Repetition rate increments were 10Hz.

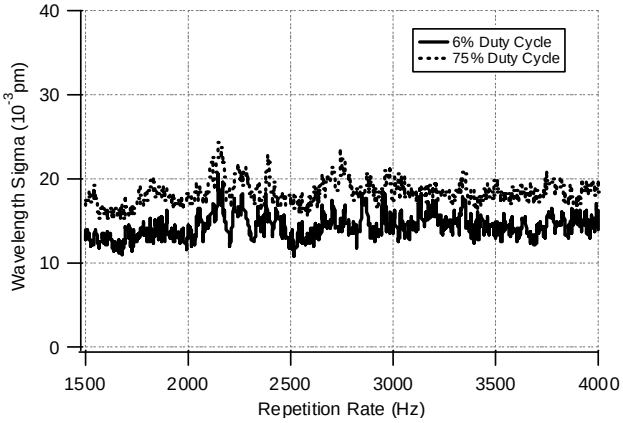

Figure 6: Wavelength sigma vs repetition rate during the same scans as in Figure 5.

Including wavelength fluctuation, repetition rate, and duty cycle effects, the XLA-200 typically produces apparent spectral bandwidths of 0.12pm in FWHM and 0.25pm in E95%. Figure 5 shows a typical bandwidth performance during repetition rate scans from 1500Hz to 4000Hz at two different duty cycles, and Figure 6 shows the average wavelength sigma data taken during the same repetition rate scans. Bandwidth measurements were done with a high resolution grating spectrometer with the integration time of 50msec, and the raw spectra were post-processed by a FFT-based spectral deconvolution routine. The laser output energy was set to 13mJ per pulse. The average wavelength sigma in Figure 6 is 17fm, from which the single pulse bandwidth is estimated to be 0.10pm. The FWHM increases due to chamber acoustic resonance are less than 0.01pm in Figure 5, and the E95% increases are contained within 0.03pm. The duty cycle effect on FWHM is negligible whereas the E95% has 0.01 – 0.03pm increases at higher repetition rates because optical power loading increases linearly with repetition rate and thus affects bandwidth.

LASER GAS CONTROL SYSTEM

Efficiency of the ArF excimer laser is a function of the ratio between argon and fluorine partial pressures for a given total laser gas pressure. The output spectral profile of the line-narrowed MOPA laser is determined by mainly two factors; the spectral profile of MO output, and the delay between MO and PA discharges (dtMOPA), which also strongly affects system output efficiency and hence must be always maintained at its optimum value to minimize pulse-to-pulse energy fluctuations due to discharge timing errors. The MO fluorine concentration is the primary factor determining the MO output bandwidth and energy efficiency. The MO output spectrum is not temporally uniform. In the MOPA configuration the temporal amplification of the MO output beam by the PA chamber does not take place uniformly, and dtMOPA plays a deterministic role in the way the MO temporal profile is amplified as it propagates through the PA gain region, hence the time integrated spectral bandwidth. Therefore, the fluorine concentrations of the two chambers and dtMOPA need to be controlled to achieve stable MO and system efficiencies, minimize pulse-to-pulse energy fluctuations, and stabilize system output bandwidth.

The XLA dual chamber laser gas control system is redesigned for stable optical performance in both short and long terms. The new laser gas control includes an improved laser gas refill procedure and totally redesigned fluorine gas injection algorithm. The new refill procedure provides a precise control of laser gas mixing ratios and total fill pressures of the two chambers, and it ensures the same gas fill condition for every gas fill. Uncertainties in the gas mixing ratios and total pressures after gas refill are reduced from approximately 3% to less than 1%. The XLA-200 fluorine gas injection control monitors dtMOPA, MO output energy, and discharge high voltage to decide the times and amounts of fluorine gas injections. It includes duty cycle and target energy compensations so that accurate injection decisions can be made in any operating condition; because all three parameters (dtMOPA, MO output energy, and voltage) are

affected by duty cycle and target energy, wrong injection decisions may be made if the operating condition effects are not properly factored in.

Data from a gas test using one of the standard manufacturing gas test protocols are shown in Figures 7 and 8. Laser operation duty cycle and target output energy are varied as shown in Figure 8 in order to test the capability of the algorithm's duty cycle and target energy compensations. The first and last 35Mpulse periods are run in the same operating condition (75% duty cycle and 10mJ output) so that an apples-to-apples comparison of the relevant parameters such as bandwidth, HV, and Emo can be made between the beginning of the gas test and the end of the gas test.

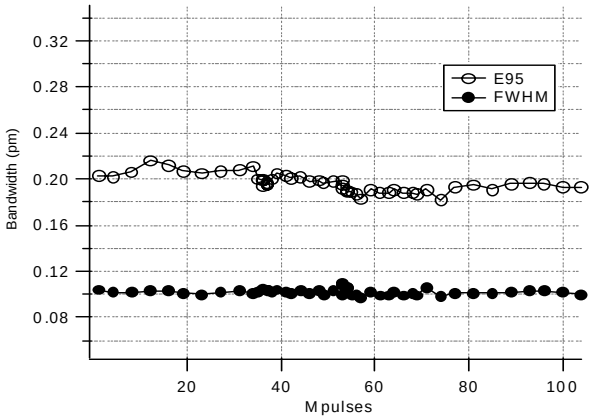

Figure 7: FWHM and E95% measured over 100Mpulses by a high resolution grating spectrometer and deconvolved by an FFT-based deconvolution algorithm.

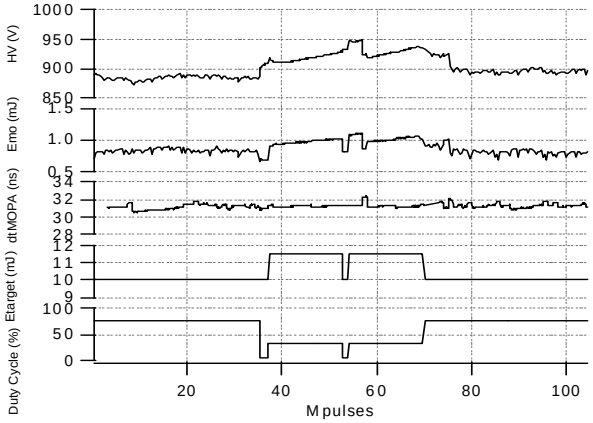

Figure 8: HV, Emo and dtMOPA recorded during a 100Mpulses gas test. Also, showing the test modes used during the test.

FWHM bandwidth drift was less than 0.01pm and E95% drift was less than 0.02pm when the initial measurements and the last measurements are compared, which is a result of the stable HV, Emo, and dtMOPA enabled by the new fluorine injection control.

BANDWIDTH ANALYSIS MODULE

The new LNM and redesigned gas control of the XLA-200 provide narrower and more stable spectral bandwidth performance. A newly designed Bandwidth Analysis Module (BAM) capable of reporting both FWHM and E95% bandwidths of the output radiation with high accuracy is incorporated into the XLA-200. Laser on-board bandwidth metrology tools normally employ fixed-gap etalon spectrometers because of their small sizes. Because this method often relies on the measurement of very small changes in the width of the spectrometer fringe, seemingly insignificant effects such as changes in input spectral shape, center wavelength, spatial line-center chirp and spatial bandwidth inhomogeneity, input optical power variations, and aging of optical components can all affect the reported bandwidth. The BAM design incorporates special features to minimize reporting errors due to those changes. Exclusive methods for homogenization of the laser radiation and for determining the light source bandwidth from the shape of the spectrometer fringe provide a high degree of accuracy in both FWHM and E95% bandwidth reporting, independent of operating wavelength.[5]

Test data are shown in Figures 9 and 10. Bandwidth modulations were obtained by varying repetition rate, dtMOPA, and wavefront. The standard deviation of FWHM tracking error between BAM and grating spectrometer measurements was 5.4 fm. The sigma of E95% tracking error was 4.4 fm. The BAM has demonstrated its capability reporting FWHM and E95% bandwidths over wide ranges of bandwidth.

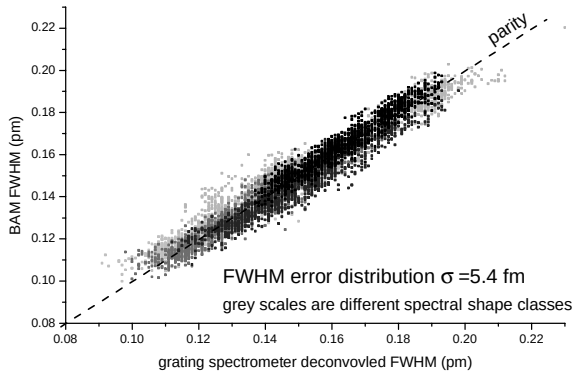

Figure 9: Demonstration of FWHM reporting error of BAM compared to high-resolution grating spectrometer for simultaneous measurement (300 pulse bursts).

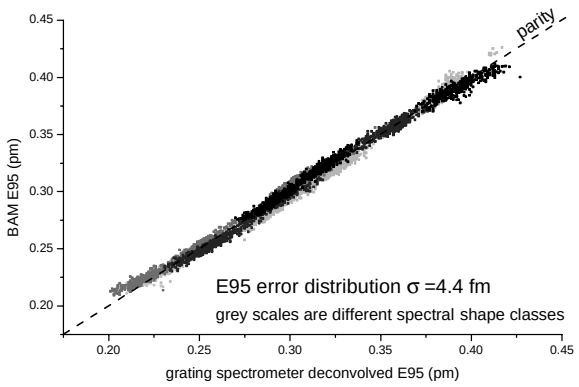

Figure 10: Demonstration of E95%% reporting error of BAM compared to high-resolution grating spectrometer for simultaneous measurement.

OUTPUT POLARIZATION AT HIGH POWER OUTPUT

The excimer laser light spectrally-narrowed by a dispersion grating naturally has a high degree of polarization with the electric field in the direction normal to the grating grooves because the grating reflectivity in that direction is much higher than in the direction parallel to the grating grooves. However at very high power levels, CaF2 optical elements may exhibit thermally induced birefringence, and polarization degrades. In addition to the thermally induced birefringence, CaF2 materials may have residual birefringence, and even minute mechanical stresses can induce birefringence. At Cymer, the ArF laser optical elements made of CaF2 that transmit high power laser pulses are carefully tested and characterized for birefringence in manufacturing, and they are installed at the preferred orientation for minimum induced birefringence that is determined during the manufacturing test process so that undesirable birefringence effects on polarization are minimized to ensure a high degree of polarization even at the maximum laser output power. In addition, optics mounts are designed to minimize mechanical stresses on optics. Polarization ratio measurements done on an XLA-200 laser are plotted against laser system output energy in Figure 11, which shows that the thermally induced birefringence is well controlled and its effect on polarization ratio is less than 1 percent.

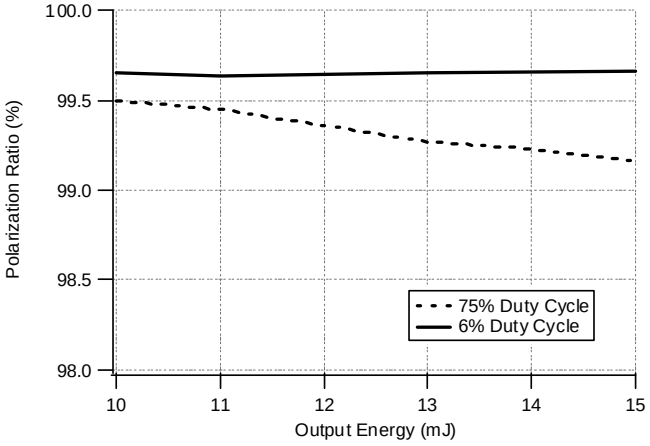

Figure 11: Polarization ratio vs output energy measured at 4000Hz on an XLA-200 laser.

MODULES LIFETIMES IMPROVEMENTS

Improvements in lifetimes of major consumables are achieved for the XLA-200. Table 1 lists major consumables lifetimes of the XLA-200.

Modules	Expected Lifetimes
PA chamber	24 Bpulses
MO chamber	12 Bpulses
LNM	30 Bpulses
LAM	30 Bpulses
BAM	30 Bpulses

Table 1: A list of XLA-200 major consumables with their expected lifetimes.

Our continuing research on electrode erosion mechanism and electrode materials has successfully provided a 30% increase to the PA chamber lifetime, and it now lasts 24 Bpulses. Optics modules have also received substantial lifetime improvements. Two on-board metrology modules, LAM and BAM, are expected to last 30 Bpulses, which are 50% increases from the previous generation products. The line-narrowing module is also expected to last 30 Bpulses. Thus, the XLA-200 provides overall a 20% reduction in the cost of consumables (COC) compared to the COC of the previous generation MOPA products.

CONCLUSION

The 193nm lithography has been widely adapted as the standard lithography process for critical layers. In the near future, the immersion lithography will play a crucial role in the volume production at 65 and 45 nm nodes. Smaller CDs and the process controls required for such CDs require a stable output spectrum, higher power output, and high degree of polarization. The XLA-200 meets those requirements with a lower cost of consumables.

REFERENCES

1. R. Sandstrom, A. Ershov, V. Fleurov, "MOPA Laser Architecture for High Power Lithographic Light Sources" SPIE 27'th Conference on Microlithography, March 3-8, 2002, Santa Clara, A*C, USA*
2. V. Fleurov, et al., "Dual Chamber Ultra Line-Narrowed Excimer Light Source for 193nm Lithography", Optical Microlithography XVI, 2003, SPIE, Volume 5040, pp1694-1703.
3. T. Ishihara, et. al., "Long-term Reliable Operation of a MOPA-based ArF Light Source for Microlithography", Optical Microlithography XVII, 2004, SPIE, Volume 5377, pp1858-1865.
4. T. Matsuyama, et. al., "Nikon Projection Lens Update", Optical Microlithography XVII, 2004, SPIE, Volume 5377, pp730-741.
5. R Rafac, "Overcoming limitation of etalon spectrometer used for spectral metrology of DUV excimer light sources", Optical Microlithography XVII, 2004, SPIE, Volume 5377, pp846-858.
6. D.G. Flagello, et. al., "Optical Lithography in the sub 50nm region", Optical Microlithography XVII, 2004, SPIE, Volume 5377, pp21-33.
7. B. Lin, "Immersion lithography and its impact on semiconductor manufacturing", Optical Microlithography XVII, 2004, SPIE, Volume 5377, pp46-67.
8. B.W. Smith, et. al., "Benefiting from polarization-effects on high NA imaging", Optical Microlithography XVII, 2004, SPIE, Volume 5377, pp68-79.